# Antibiotic Releasing Biodegradable Sutures for the Prevention of Surgical Site Infections

BEE 4530

Caitlin Bowen, Calvin Kersbergen, C. Garrett Rappazzo, Beth Weed

## Table of Contents

## 1.0 Executive Summary

Although a necessary component of surgery, sutures have been shown to exhibit an affinity for microbial adherence and colonization. The sutures offer a conduit for bacteria directly into the wound and infection can be difficult to treat post-colonization, even with antibiotics that are traditionally very effective. Infections associated with sutures are often difficult to resolve and require extended hospitalization, therapy, or additional surgical procedures. Drug eluting sutures offer a potential solution to this issue. In order to maximize antibiotic delivery, modeling changes in suture size, placement, and concentration could provide valuable information for surgeons and manufacturers to better develop and implant sutures, reducing the number of surgical site infections (SSIs) and thus morbidity and mortality.

Using COMSOL software, we first generated both a 2D and a 3D model of MONOCRYL plus antibiotic sutures in the skin. Next, we modeled antibiotic-release and biodegradation by tracing the distance the drug penetrates into the surrounding tissue while the suture and the antibiotic are simultaneously being degraded by the body's enzymatic processes. Finally, we adjusted the distance between adjacent sutures and suture size to ensure that the minimum inhibitory concentration (MIC) of triclosan for various bacteria strains was met at the wound site, without increasing the difficulty for surgeons to implant the suture.

In our model, we showed the dispersion of antibiotics into the surrounding tissue over time, demonstrating up to what time point the sutures are able to maintain at least the minimum effective concentration level of antibiotic. We show that antibiotic levels sufficient enough to inhibit bacterial growth can be reached in complex environments, such as the skin. Based on our 3D model, the maximum spacing between adjacent 4-0 sutures to maintain a MIC for *S. aureus* for 72 hours after suture implantation is 2 mm. Suture spacing for other strains of bacteria can be determined through our predictive equations. The duration of antibacterial properties increases as the spacing between sutures is decreased, but increasing the initial concentration of triclosan in the suture does not significantly increase the duration of antibacterial properties of the suture. The suture decreases in volume by 45% seven days after implantation in the skin, indicating proper surface erosion and a significant loss in tensile strength after that time. The integrity of the suture is necessary to keep the wound closed over the entire healing period, preventing bacteria from entering through the open site and entering the tissue and subsequently traveling through the bloodstream.

In this model, we reinforce *in vivo* and *in vitro* studies that suggest the effectiveness of antibiotic releasing sutures by modeling antibiotic concentrations in the skin following suture placement. This model will help surgeons determine the spacing for a variety of commercially available sutures, based on the bacterial inhibition properties required, in an effort to reduce the number of surgical site infections that occur. By ensuring effective distribution of antibiotic, following our developed standards in the surgical suite will reduce the number of surgical site infections, significantly reducing costs, morbidity, and mortality from post-operative infections.

## 2.0 Problem Statement

Surgical site infections (SSIs) can result in significant post- surgical complications, such

as preventable infections or sepsis, as well as increased treatment duration and cost. Sutures embedded with antibiotic are currently the strongest method for preventing bacterial growth and infection at a wound site. However, if the antibiotic concentration in the skin at the wound site is not high enough over the period of time it takes for the wound to heal, the antibiotic provides no benefit to the patient and infection is likely to occur. The optimal suture type, suture spacing, and suture size must be determined for surgeons to optimize effectiveness of the antibiotic in the surgical suite and post-operatively.

## 3.0 Introduction

### 3.1 Background

The estimated incidence rate of SSIs is 2.8% in the United States, with significant morbidity and mortality as well as increases in patient cost and duration of hospital stay (1). Approximately 750,000 people contract SSIs each year, costing the healthcare industry over one billion dollars (1). Recent advances in drug-eluting degradable sutures allow for antibacterial release into tissue following implantation, offering a promising solution to reduce the number of SSIs. However, it is difficult to determine correct suture spacing and suture size for optimal delivery of antibiotic through an *in vitro* or *in vivo* model.

### 3.2 Literature Review

Infections associated with sutures are often difficult to resolve, require extended hospitalization, therapy, or additional surgical procedures. Although a necessary component of surgery, sutures have been shown to exhibit an affinity for microbial adherence and colonization (2). Sutures can serve as a conduit for bacteria directly into the wound, and infection can be difficult to treat post-colonization, even with antibiotics (3). The physical configuration of a suture is an important factor in the susceptibility of a wound to infection. Sutures come in two configurations, monofilament and multifilament, which may be twisted or braided. With comparison to monofilament sutures, multifilament sutures have greater ease of handling and provide greater knot security, thereby decreasing the risk of premature suture failure. However, it has been found that sutures in a multifilament configuration harbor bacteria between adjacent fibers and the fibers allow for bacteria to migrate freely along the suture through capillary action (4). This leads to both higher degrees of local inflammation tissue reactions and higher rates of wound infection (4, 5). For this reason, monofilament sutures are frequently chosen for wounds not incurred within a sterile field.

Monofilament sutures can be absorbable (biodegradable) or non-absorbable. Absorbable sutures confer the advantage that they will degrade as the tissue heals, eliminating follow-up with a clinician to remove the sutures and preventing any foreign-body reactions. However, unlike non-absorbable sutures, absorbable sutures lose their strength over time, which may compromise the wound's healing process. Efforts have been made to respond to this issue, increasing the strength retention over time. MONOCRYL, a monofilament absorbable suture, has been shown to retain 20-30% of its initial tensile strength two weeks after implantation yet be completely resorbed after three months (6, 7). In locations where tissue healing is rapid, like at the skin surface, absorbable sutures are the ideal choice. For these reasons, biodegradable sutures

are typically used at wound sites in an effort to limit the number of doctor visits and prevent foreign-body reactions. Non-absorbable sutures can elicit foreign body reactions, leading to increased inflammation and infection, and must be physically removed from the patient following wound healing (8).

To further prevent bacterial infection, biodegradable sutures can be impregnated with an antibiotic. For example, Ethicon's MONOCRYL Plus sutures (poliglecaprone 25) with triclosan, an antibacterial drug, have been shown to prevent bacterial growth *in vitro* for up to 11 days (3). Degradable sutures also confer the advantage that they allow for nearly constant release of antibacterial components within the suture. According to Ming, *et al*. (2007), MONOCRYL Plus Antibacterial Sutures are effective *in vitro* at prohibiting bacterial growth, each species with a unique zone of inhibition that depends on the robustness of the strain tested (Figure 1) (3).

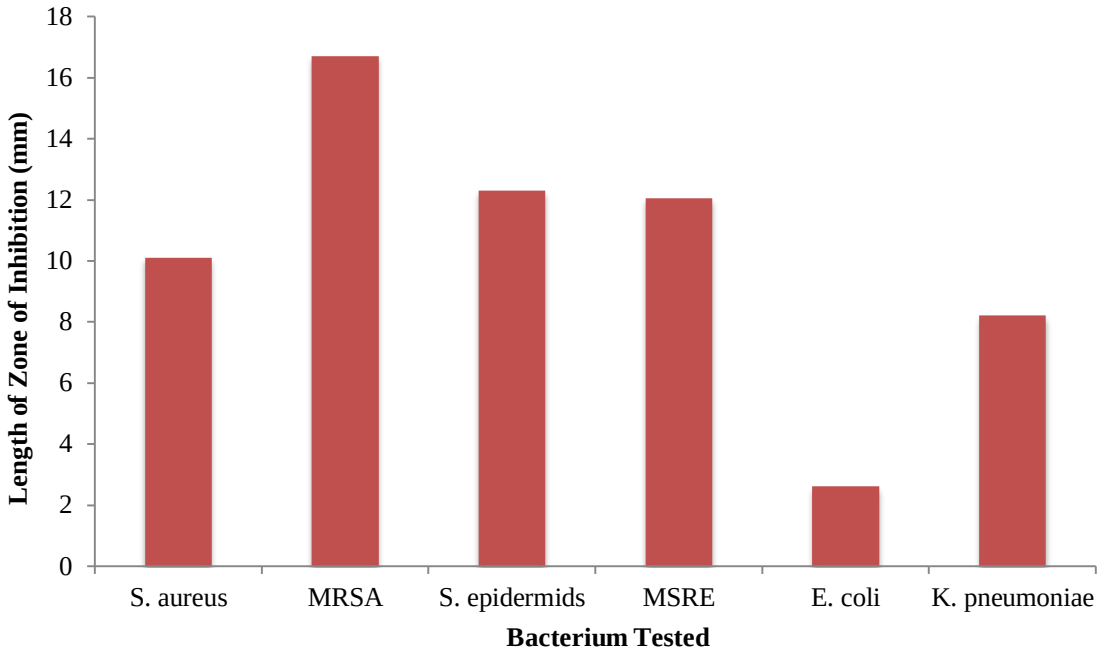


Figure 1. *In vitro* efficacy of poliglecaprone 25 suture with triclosan (MONOCRYL plus), adapted from Ming *et al* (2007). Efficacy was determined by the length of the zone of inhibition, i.e. the higher the zone of inhibition, the more effective the suture was at preventing bacterial growth in a Petri dish. MRSA: methicillin-resistant *S. aureus*; MRSE: methicillin-resistant *S. epidermidis* (3).

The pathogens most commonly found in surgical site infections are *S. aureus*, *S. epidermidis*, along with *E. coli* and *K. pneumoniae*. Figure 1 demonstrates that triclosan-eluting sutures are effective at inhibiting all of these bacterial strains. Jones *et al* (2006) determined the MICs of triclosan, a broad-spectrum antibiotic, for different strains of bacteria (9). For most strains of *E. coli*, the triclosan MIC is 0.2 mg/L. For *S. aureus*, the triclosan MIC for the most resistant strain is 0.4-0.6 mg/L (9). We use these values as targets for concentrations in the wound area and surrounding skin, as they will be necessary to achieve in order to inhibit bacterial growth at the suture and wound site.

Despite the promise of antibiotic releasing biodegradable sutures, it is a necessity that these sutures be sewn properly, in both depth and stitch distance, by the surgeon for optimal antibiotic delivery to the surgical site (3). Furthermore, the metabolism of triclosan in the skin

must be considered to ensure effective antibiotic properties. In the skin, triclosan is metabolized into triclosan glucuronide and triclosan sulfate via skin glucuronyltransferases and sulfotransferases, respectfully, mostly in the outer root sheath of the hair follicles, sebaceous glands, and stratum basale (10). The metabolism of triclosan decreases the amount that can potentially reach the wound site, however the rate of degradation is not very significant compared to the inhibitory concentration levels that need to be reached.

We will use Ethicon's MONOCRYL plus antibiotic as the basis for our model, as it is biodegradable monofilament suture containing triclosan and has been shown to be effective against the most common SSI pathogens. The software COMSOL will provide a modeling platform that will allow us to optimize suture placement, size, and antibiotic concentration without performing many experiments *in vitro* or *in vivo*. We will model the diffusion of antibiotic from MONOCRYL Plus sutures with degradation in the skin to demonstrate the optimum suture placement and size at the wound site in order to prevent bacterial infection and growth at the wound.

### 3.3 Problem Schematic

To model suture placement and antibiotic concentration profiles in the skin following surgery, we first developed a two-dimensional model of the suture. The geometry of the model is axisymmetric around the wound, and only half of the suture is shown due to symmetry (Figure 2). The far-right boundary is set to have a concentration of antibiotic equal to zero, as any antibiotic at this location of the skin is immediately taken away by the bloodstream.

However, this boundary is not consistent in the two-dimensional axi-symmetric model, as the surface of the skin does not contain blood vessels and therefore the $c_T = 0$ boundary condition on the far right of the 2D model is not accurate at all locations around the axis. A semi-infinite boundary condition here, which was also considered, is also not accurate, as the skin is not deep enough for a true semi-infinite boundary. Thus, we extended our model to three dimensions, which also allowed us to take into effect the diffusion of triclosan from the external portions of the suture into the skin (Figure 2). Furthermore, we were able to more accurately represent the stitch pattern in the skin using a 3D model, as the pattern is not perfectly circular and there is a significant portion of the stitch outside the skin that is not degraded by enzymes. This portion of stitch outside of the skin can still contribute to drug elution profiles within the skin. We also implemented a partition coefficient between the stitch and the skin, which is not shown on the schematic in Figure 2. Triclosan is degraded at a first order rate in the skin.

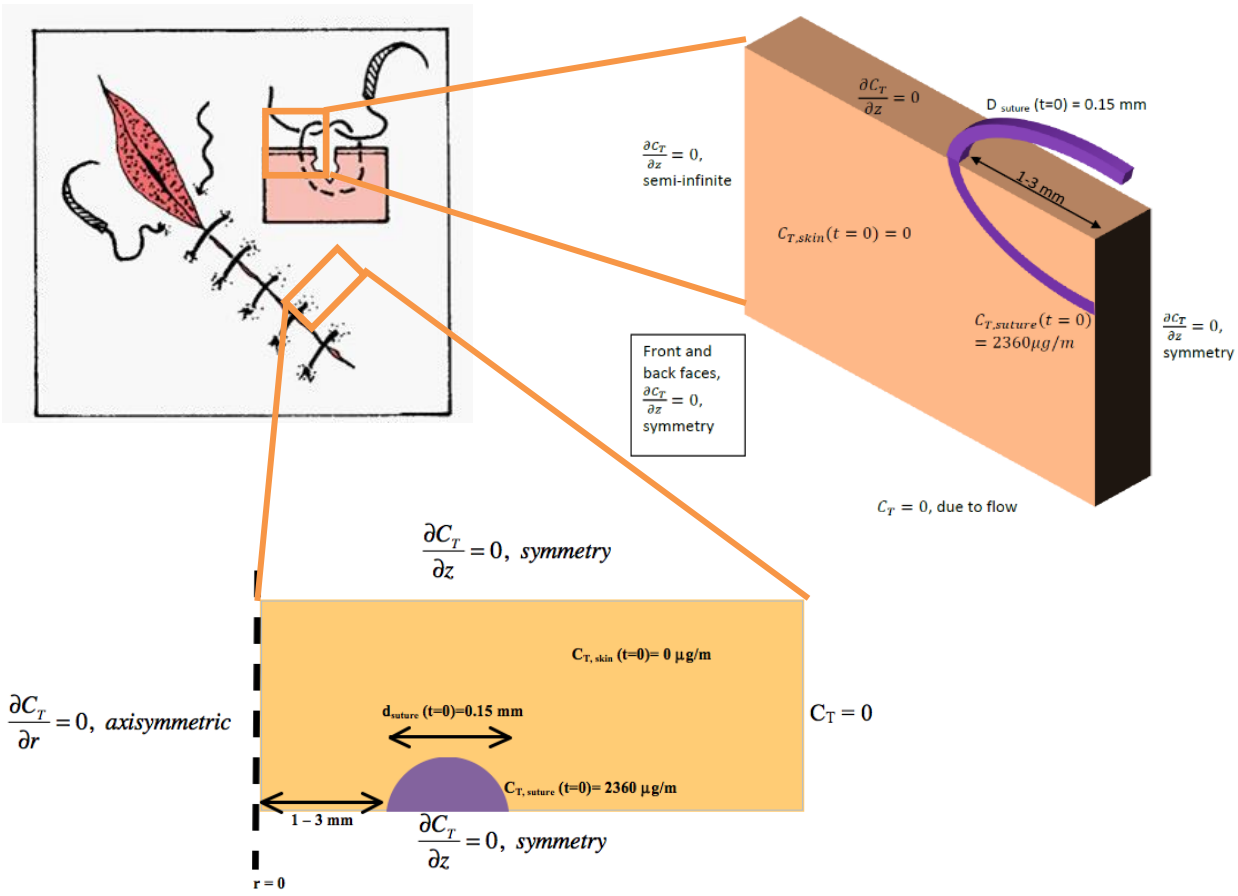


Figure 2. Diagram depicting suture placement (top) and model schematic in 2D (bottom) and 3D (top). Purple – Suture (MONOCRYL-PLUS); Yellow – Epidermis

We first used the 2D model to determine whether antibacterial concentrations high enough to inhibit bacterial growth can be reached in a timely manner and to show degradation of the suture in the skin. Next, we used our 3D model to optimize the distance between adjacent sutures for several suture sizes based on antibiotic concentration, helping surgeons to choose the best size and stitching pattern to confer bacterial resistance in the wound following surgery.

### 3.4 Design Objective

The goals of this report are to model both the dispersion of antibiotics from an implanted suture and absorption of suture from the surrounding tissue, as well as optimize the placement of sutures of various sizes to identify an ideal elution profile for combating bacterial infection and provide surgeons and physicians with guidelines for suture implantation in the surgical suite, reducing costs, morbidity, and mortality.

**4.0 Governing Equation**

In our 2D model, we calculated mass transfer in cylindrical coordinates with a first order degradation term within the skin. Equation 1 describes the transport of triclosan ($C_T$) in the skin and equation 2 describes the transport of triclosan in the suture with changes in time. Equations 3 and 4 describe the transport of triclosan in the skin and the suture, respectively, in our 3D model with the same conditions.

$$\frac{\partial C_T}{\partial t} = D_{skin}\left(\frac{1}{r}\frac{\partial}{\partial r}\left(r\frac{\partial C_T}{\partial r}\right)+\frac{\partial^2 C_T}{\partial z^2}\right)+R_{skin} \quad \text{(Eq. 1)}$$

$$\frac{\partial C_T}{\partial t} = D_{suture}\left(\frac{1}{r}\frac{\partial}{\partial r}\left(r\frac{\partial C_T}{\partial r}\right)+\frac{\partial^2 C_T}{\partial z^2}\right) \quad \text{(Eq. 2)}$$

$$\frac{\partial C_T}{\partial t} = D_{skin}\left(\frac{\partial^2 C_T}{\partial x^2}+\frac{\partial^2 C_T}{\partial y^2}+\frac{\partial^2 C_T}{\partial z^2}\right)+R_{skin} \quad \text{(Eq. 3)}$$

$$\frac{\partial C_T}{\partial t} = D_{suture}\left(\frac{\partial^2 C_T}{\partial x^2}+\frac{\partial^2 C_T}{\partial y^2}+\frac{\partial^2 C_T}{\partial z^2}\right) \quad \text{(Eq. 4)}$$

The surface erosion of suture is modeled by equation 5:

$$\frac{dr}{dt} = K \quad \text{(Eq. 5)}$$

Where K is the surface erosion rate of the suture, 7 μm/day and r is the radius of the stitch (11).

The growth of skin to replace degrading suture uses the same erosion rate as the suture (Equation 6).

(Eq. 6)

Where K is the surface erosion rate of the suture, 7 μm/day, and r is the stitch radius (11).

Equations 5 and 6 were adapted in the model to account for erosion and growth in all three dimensions by multiplying each dimension by the vector normal to the suture surface.

As triclosan diffuses through the tissue, it is metabolized. The metabolism of triclosan in the epidermis is modeled with Equation 7.

$$R_{skin} = kC_T \quad \text{(Eq. 7)}$$

Where k is the first order reaction coefficient, -3.18944 x $10^{-6}$ mol/$m^3$/s and $C_T$ is the concentration of triclosan in the skin (10).

## 5.0 Boundary Conditions

2D: On the left-hand boundary, the flux is zero due to two-dimensional axi-symmetry. The right-hand boundary has the concentration of antibiotic equal to zero, due to triclosan being taken away by the bloodstream. On the top and bottom boundaries, the flux of triclosan is zero due to symmetry.

3D: The bottom of the skin has a concentration of zero due to drug being taken away by blood flow at the base of the dermis. The left, front, and back sides have a flux of zero due to symmetry. The top is set to an open boundary of zero flux. The right side is considered semi-infinite because it is far away from the suture in the skin, and so has a flux of zero.

## 6.0 Initial Conditions

The concentration of triclosan in skin before the suture is placed is zero. The suture diameter is originally 0.15 mm, corresponding to a size 4-0 suture (3). The initial suture concentration is 2360 μg/m, which we determined using the cross-sectional area of the suture to be 4.612 mol/$m^3$ (12). These initial conditions are accurate for both 2D and 3D models.

## 7.0 Results and Discussion

Triclosan diffuses very quickly away from the suture due to the large differences (approximately three orders of magnitude) in the diffusivity of triclosan within the suture and in the skin (Figure 3A). The 2D model shows that triclosan has its peak concentration between the sutures at the wound site, where bacterial colonization is most likely to occur (Figure 3B). The MIC desired for *E. coli* is 6.91 x $10^{-4}$ mol/$m^3$ and the MIC for *S. aureus* is 2.07 x $10^{-3}$ mol/$m^3$.

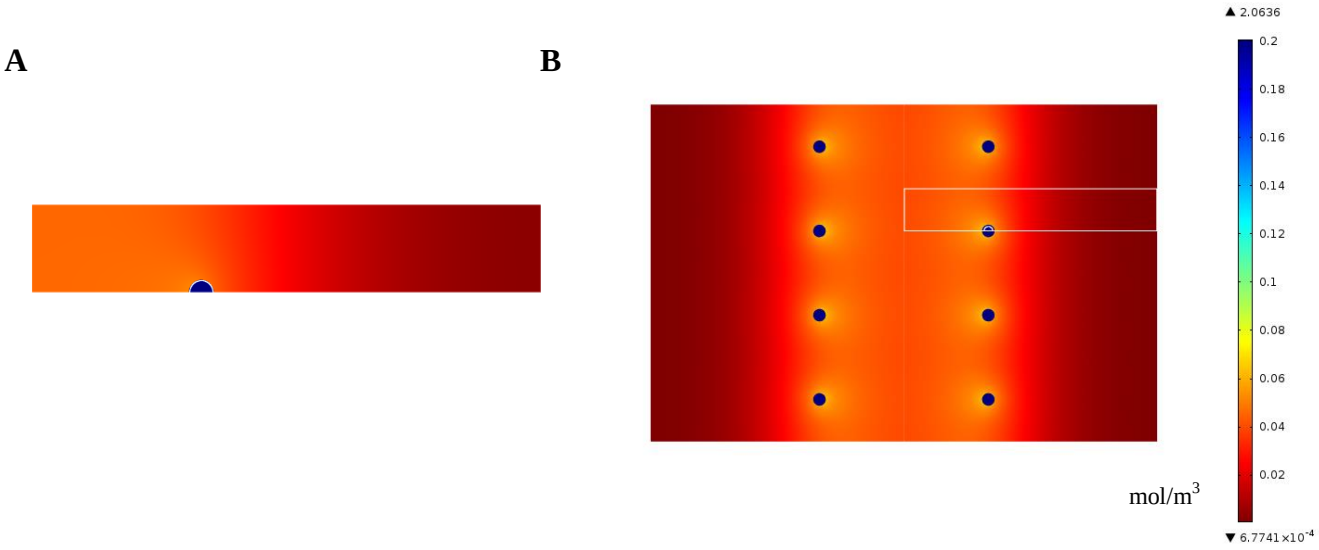


Figure 3. Triclosan concentration profile in 2D at 3 hours, in mol/$m^3$. A) Concentration within the computational domain. B) Representation of several sutures over a central wound region, where the wound is approximated as the centerline between the sutures.

In the 2D model, the concentration reaches its peak at the center of the wound site 1 mm between adjacent sutures at approximately 4 hours after suture implantation at a concentration of 0.045 mol/m$^3$, well above the MIC for both *E. coli* and *S. aureus*. (Figure 4A). Within the center of the suture, the triclosan concentration is about half of its initial suture concentration after one day and drops away to 0 mol/m$^3$ rapidly (Figure 4B). It is crucial that the concentration peaks within the 24-hour window, as that is when bacterial infection is most likely to occur. After a biomaterial has been present for 24 hours, the risk of infection decreases significantly (13).

**A** **B**

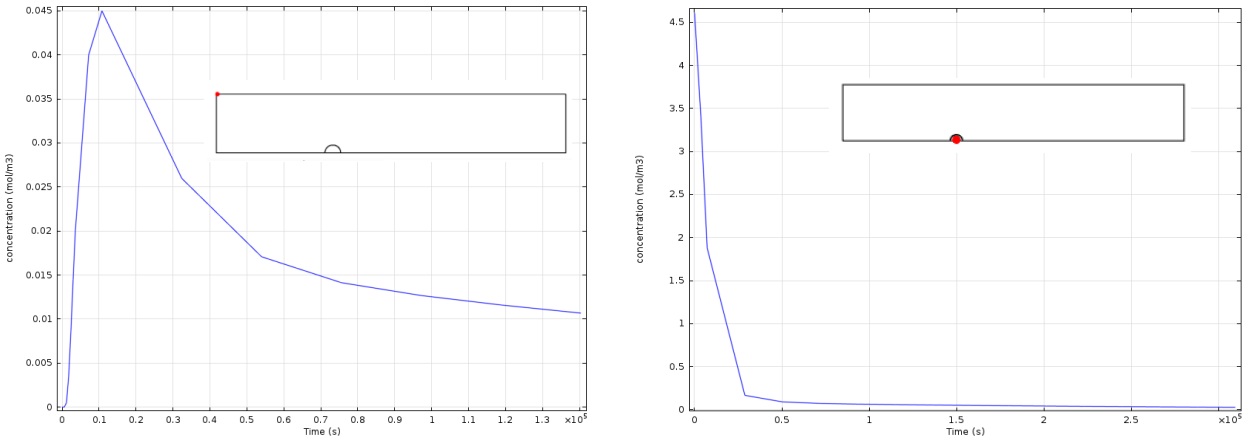


Figure 4. Concentration profile (mol/m$^3$) over 48 hours (A) Between sutures at center within the wound (B) Within center of suture.

Our 2D model shows that concentrations of triclosan high enough to inhibit bacterial growth are reached in the skin surrounding the suture. However, because of the zero concentration boundary condition and schematic, the 2D model only accurately represents the suture within the skin itself and does not accurately model the skin surface or diffusion of triclosan along the external portions of the suture. Hence, we extended our suture model to 3D to better encompass the effects of triclosan diffusion from the externally placed suture, as well as model the triclosan concentration profile more accurately at the skin surface. Our 3D model (Figure 6A) takes into consideration the oval placement of the suture in the skin, as well as the effects of diffusion of triclosan along the suture, degradation of the suture in three dimensions (Figure 6B), as well as diffusion of triclosan in the skin in three dimensions (Figure 6C and Figure 6D).

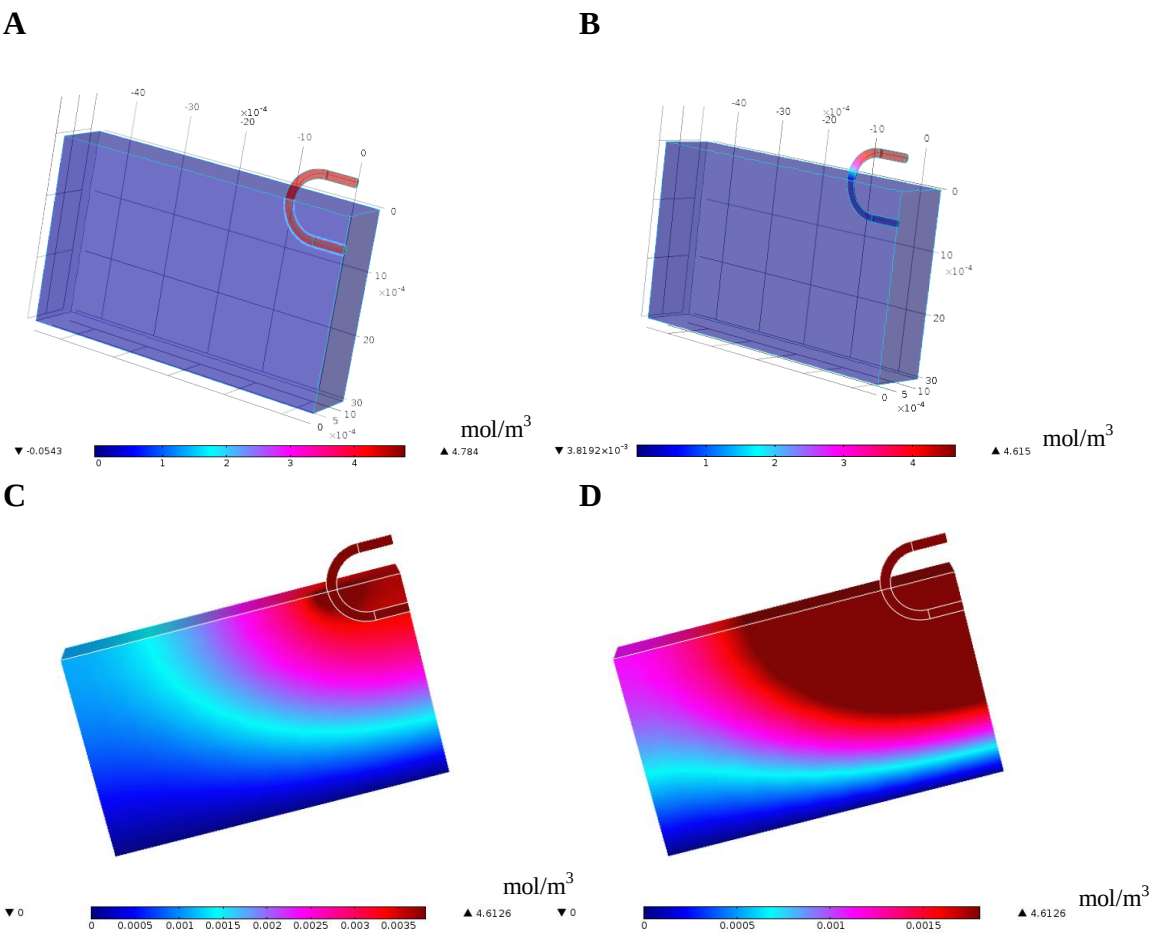


Figure 6. A) Concentration profile of triclosan after suture implantation (time t = 0). B) Concentration profile after three days. C) Modified scale (0, 3.8E-3 mol/m$^3$) to show distribution near suture after three days. D) Modified scale (0, 1.8E-3 mol/m$^3$) to show distribution of drug in skin after three days.

By evaluating the concentration profile of triclosan in the 3D model, we observed that triclosan diffusion along the suture itself contributes to increased antibiotic delivery (Figure 6C). Furthermore, we observe a gradient of triclosan, decreasing in concentration further away from the wound (Figure 6D). Diffusion from the 3D suture at a point 1 mm between adjacent sutures reaches inhibitory concentrations for the first 72 hours after implantation (Figure 7A).

**A** **B**

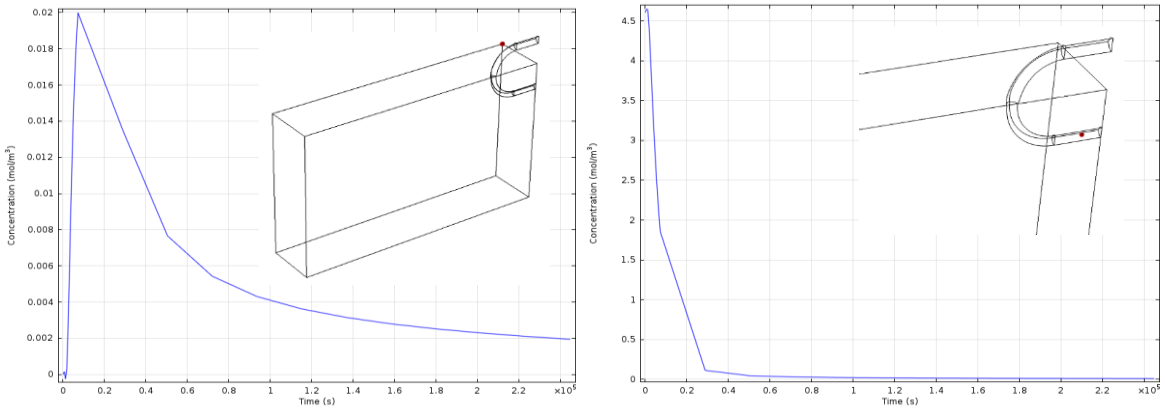


Figure 7. Concentration profile (mol/$m^3$) over 72 hours in 3D model with moving boundary (A) Between sutures at center within the wound (B) Within center of suture.

In order for complete antibacterial properties, the location furthest from the suture in the wound must reach MIC for an extended period of time. In Figure 7, we show the concentration of triclosan within the wound 1 mm from adjacent sutures reaches a maximum concentration well above the MIC for *S. aureus* after 3 hours. The concentration of triclosan in the suture drops rapidly, reaching half of the initial concentration after 3 hours and is nearly depleted after 24 hours in the skin.

The concentration of triclosan over time both between sutures and within the suture (Figure 7B) in the 3D model mirror the concentrations determined by the 2D model at the same locations. With the 3D model, we were able to incorporate drug diffusion through both the internal and the external portion of the suture (Figure 8).

**A** **B**

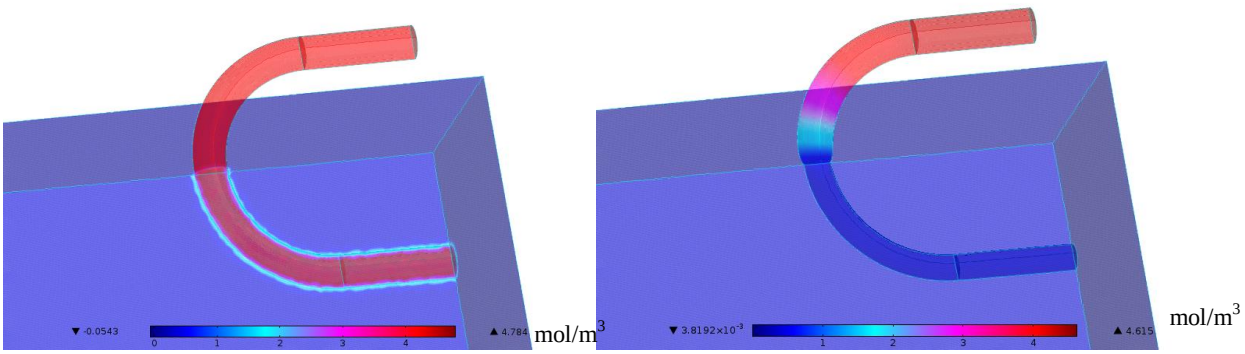


Figure 8. Degradation of the MONOCRYL suture A) at time t = 0 B) after 3 days in 3D. The suture is shrinking in the skin, and some of the triclosan is diffusing into the skin from the external portion of suture.

The 3D model is also more accurate in that the external portion of the suture is not degrading with time, as it is not exposed to enzymes within the skin (Figure 8B). To calculate degradation of the suture in the 3D skin model, we plotted the total volume of the suture over 7 days. In this time period, the suture decreases in volume by ~45% (Figure 10).

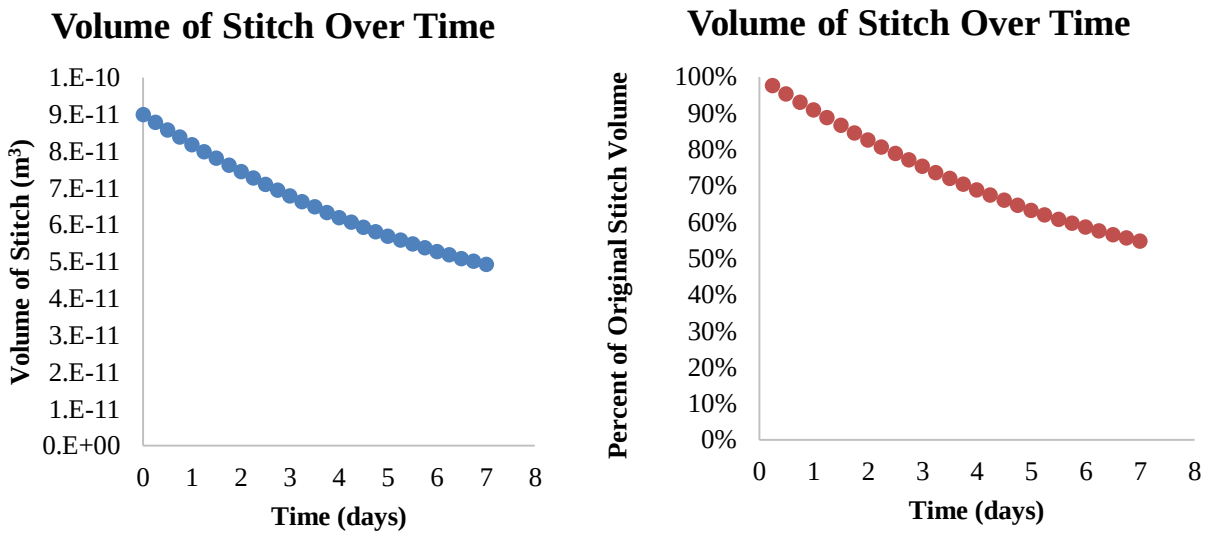


Figure 10. Total stitch volume over time. The total volume of the stitch (including both degrading and non-degrading portions) decreases over time, approaching the total volume of the stitch only outside the skin, which is not degrading. Over seven days, the total volume of the stitch decreases by about 45%.

The stitch is approaching a final volume that is 50% of the total volume, as one half of the stitch is not being degraded by enzymes as it is outside of the skin. Once the portion of the stitch inside the skin has degraded fully, the outside portion of the stitch will fall away from the wound site. Degradation of the suture allows for improved antibacterial release, reducing the amount of antibiotic that must diffuse through the suture to reach the skin.

In order to determine which of the parameters used in this model was the most sensitive to change, we performed a sensitivity analysis, varying each the diffusivity of the skin, the diffusivity of the suture and the initial concentration of antibiotics by up to 10% (Figure 11). Changes in initial concentration showed the largest percent change in concentration of antibiotics outside the suture after 72 hours. Changes in suture and skin diffusivity showed a much more insensitive response in concentration.

**A**

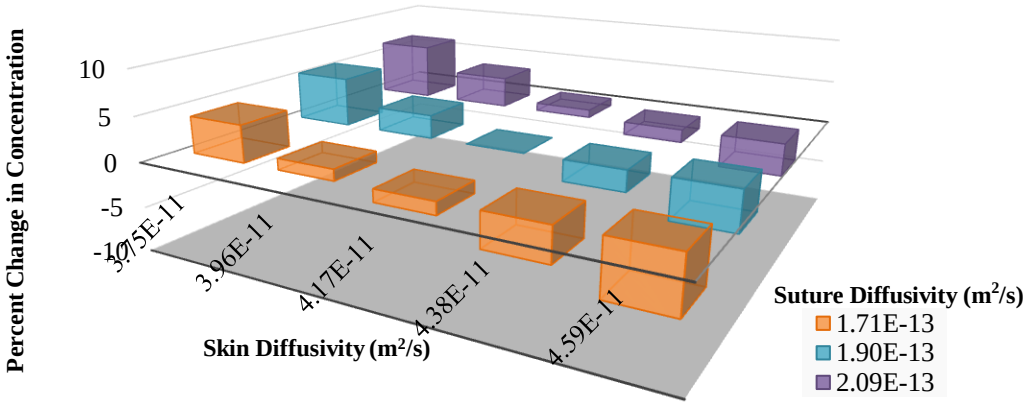


**B**

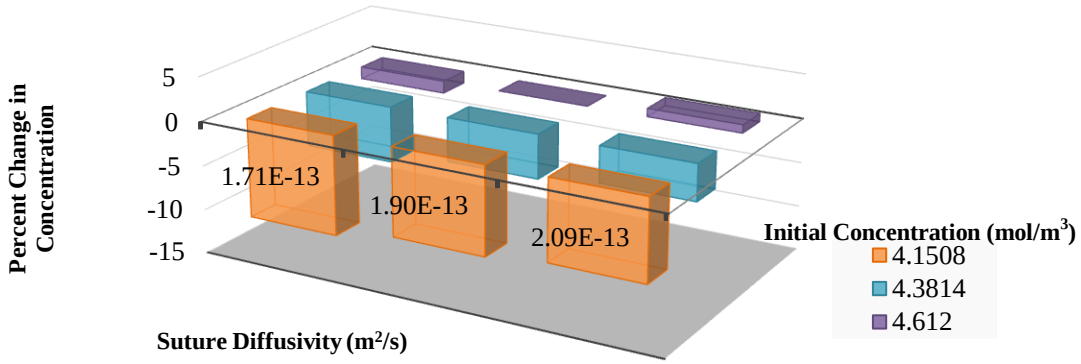


**C**

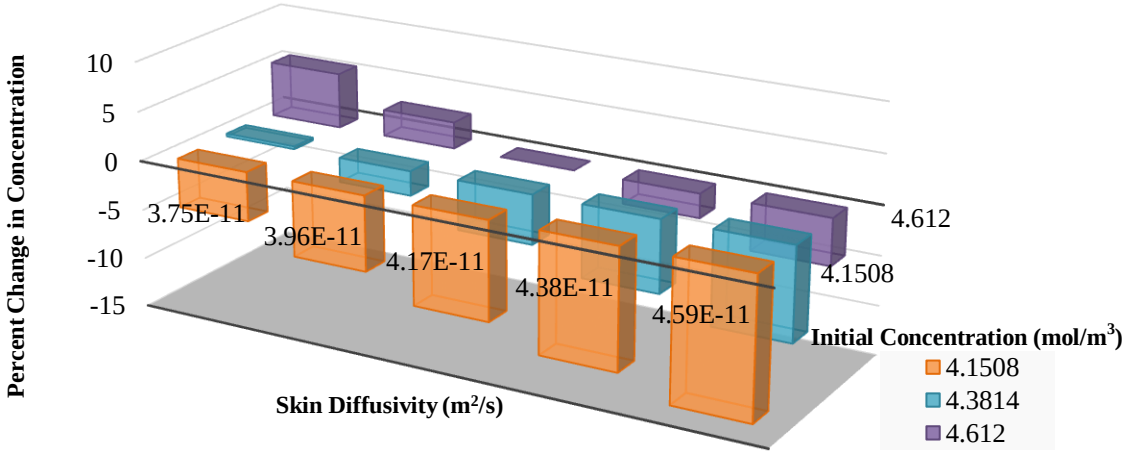


Figure 11. Sensitivity analysis to a change in drug diffusivity though the skin and suture. The bar with zero percent change represents the parameters used in the model ($D_{skin}$=4.17e-11 $m^2/s$, $D_{suture}$=1.90e-13 $m^2/s$, Initial Concentration 4.612 $mol/m^3$). The magnitude of the bars represent the percent change in antibiotic concentration just outside the suture 3 days after implantation. A) Sensitivity of concentration with respect to skin and suture diffusivity. B) Sensitivity of concentration with respect to suture diffusivity and initial concentration. C) Sensitivity of concentration with respect to skin diffusivity and initial concentration.

One of the main goals of this study was to determine the effect of suture spacing on the concentration profile of triclosan in the skin. The 3D model was run using a variety of distances between the sutures to determine beyond which spacing the minimum inhibitory concentration would not be reached 3 days after implantation. The concentration profile at a point equidistant between adjacent sutures decreases with larger distances, and spacing beyond 6mm no longer showing an initial peak and decay pattern. (Figure 12).

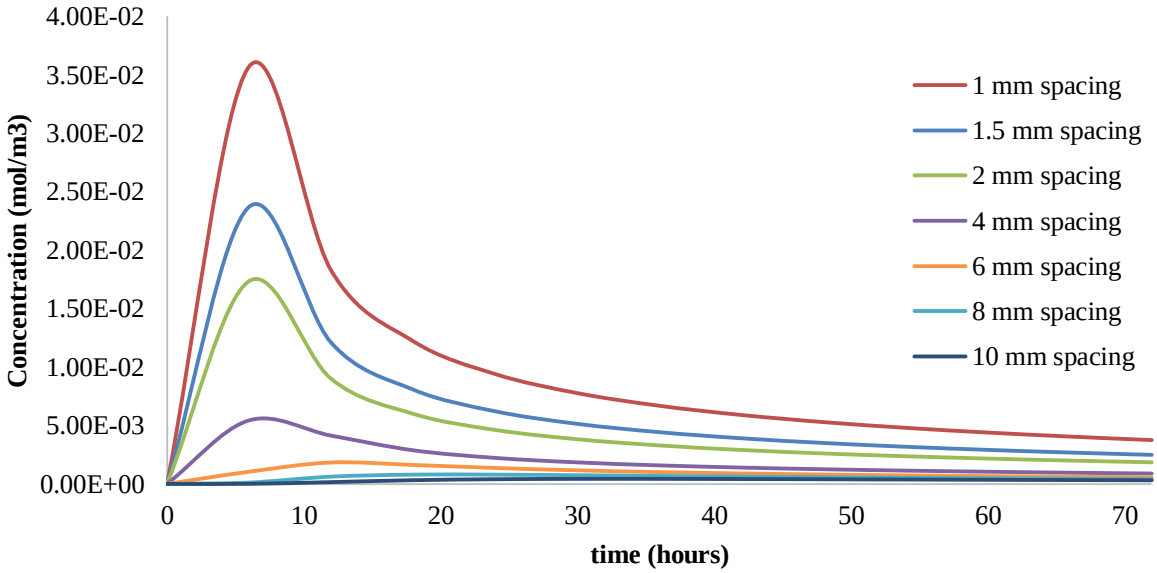


Figure 12. The effect on suture spacing on the concentration profile of antibiotics midway between the stitches, at the wound site.

As infection is most likely to occur in the first 72 hours after surgery, choosing a spacing that would be most likely to prevent infection during these critical hours is extremely important. Given that the MIC of *S. aureus* growth is 2.07 $x10^{-3}$ $mol/m^3$, our model predicts a maximum allowable spacing of 2 mm between sutures should be used during surgery for the standard size and triclosan concentration found in MONOCRYL Plus sutures (Figure 12). Given that the MIC for preventing *E. coli* growth is 6.91 $x10^{-4}$ $mol/m^3$, our model predicts a maximum allowable spacing of 4 mm between sutures should be used during surgery for the standard size and triclosan concentration found in MONOCRYL Plus sutures (Figure 13). There is a decay in the concentration at the 72 hour mark within the wound site with increasing spacing.

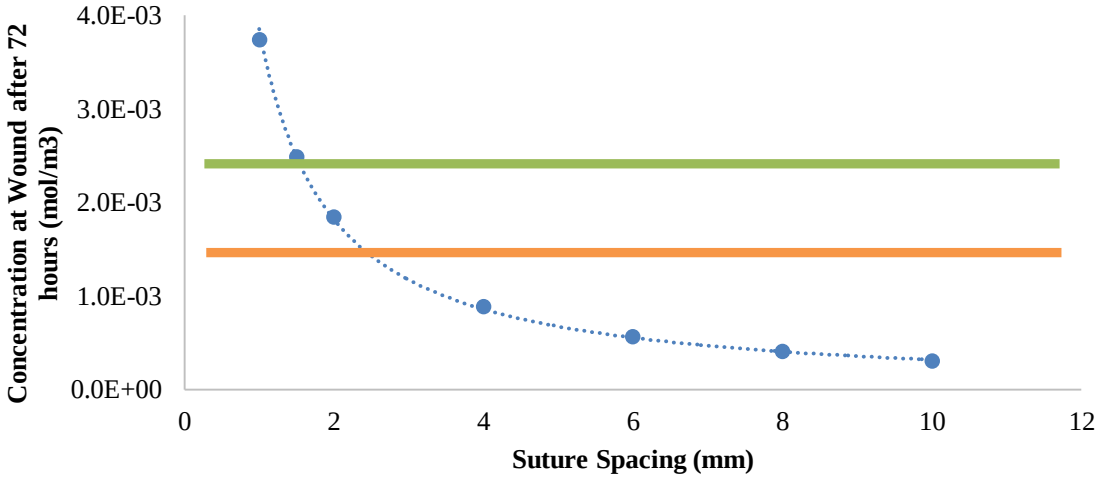


Figure 13. The effect of suture spacing on the concentration of triclosan in the center of the wound furthest from the 4-0 suture 72 hours after implantation. Horizontal lines indicate MIC concentrations for *S. aureus* (green) and *E. coli* (orange).

We repeated these calculations with different sized sutures, in order to cover a broader range of wound sizes and shapes. Different sized sutures are used in different scenarios and wound types, and we wanted our model to be used for a broad range of situations. Table 1 shows our recommended spacing to ensure MIC levels for at least 72 hours for four different suture sizes and the two most common bacterial strains.

Table 1. Recommended suture spacing for different sized sutures and different bacterial strains. Each bacterial strain has a different minimum inhibitory concentration that must be met at the wound to prevent growth.

| | **Size 5-0** | **Size 4-0** | **Size 3-0** | **Size 2-0** |
|---|---|---|---|---|
| ***E. coli*** | 2 mm | 4 mm | 6 mm | >10 mm |
| ***S. aureus*** | --- | 2 mm | 4 mm | 8 mm |

Our model showed that size 5-0 sutures are too small to prevent *S. aureus* growth, even at distances as close as 1 mm between sutures. A higher initial concentration of triclosan would be necessary in order to counteract this problem. Size 2-0 sutures are extremely large, and for weaker bacterial strains, such as *E. coli*, the surgeon can be confident that the MIC will be met for at least 72 hours, even if the stitches are further apart. However, we did not want to limit the surgeons to two bacterial strains that we picked. If a hospital is known to have a common strain or perhaps a more resistant strain of bacteria, our predictive equations can demonstrate the exact maximum spacing between sutures in order to prevent bacterial infection (Table 2). In Table 2, Y represents the MIC that needs to be met for at least 72 hours at the wound site and X represents the recommended minimum distance between sutures.

Table 2. Equations developed that predict the spacing that must be maintained in order to prevent a given minimum inhibitory concentration for different sized sutures.

| | Predictive Equation |
|---|---|
| **Size 5-0** | $y = 0.0016x^{-1.068}$ |
| **Size 4-0** | $y = 0.0039x^{-1.081}$ |
| **Size 3-0** | $y = 0.0069x^{-1.095}$ |
| **Size 2-0** | $y = 0.0169x^{-1.105}$ |

Triclosan coated sutures have been shown to significantly reduce the number of SSIs by 30% compared to uncoated sutures from the same manufacturer, especially in abdominal surgery and clean or clean-contaminated incisions in 3,720 patients (4). We have observed that the MIC for *S. aureus* was reached at the most distant point between sutures for 40 hours with 4 mm spacing between sutures. However, at larger suture separation, the MIC is reached for much shorter time periods, which may result in decreased effectiveness in antibacterial properties. Additionally, implantation of antibiotic-embedded sutures into guinea pigs and mice showed reduced bacterial colonization compared to non-antibiotic infused sutures after 48 hours.

To validate our model, we compared our results to studies modeling diffusion of triclosan through sections of cadaver skin. Studies modeling penetration and metabolism of triclosan through human and rat epidermis have shown that 24 hours following application of triclosan, 6.3% of the applied surface dose had penetrated through 200 μm skin sections and 25% of the dose remained in the skin (10). To compare across different study setups, we plotted the concentration of triclosan 200 μm away from the suture surface vs. time, normalizing the concentration values to the maximum concentration obtained. We see significant overlap at early time points between the normalized concentration in the stratum corneum and the diffusion profile from our suture model and a very similar peak and decay concentration profile (Figure 14).

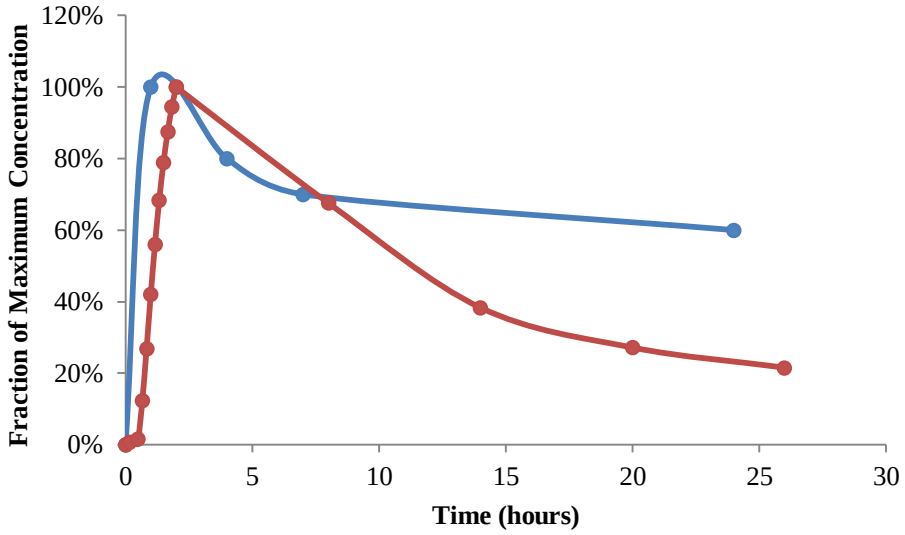


Figure 14. Diffusion profile of our 3D model (red) and Moss *et al* (1999) work on diffusion of triclosan through 200 μm segments of human stratum corneum (blue). Absolute concentrations are normalized to the maximum concentrations that are reached in the stratum corneum to account for the differences between diffusion from a suture and from triclosan applied directly to the skin.

Differences at later time points may be due to the fact that the suture begins with a finite amount of triclosan, while in the experiment carried out by Moss *et al*, triclosan remains in high quantity on the skin surface throughout the experiment. For this reason, comparing absolute or relative values is not feasible due to the different application modes. However, comparing solutions as a fraction of their maximum concentration gives insight into the diffusion profile and the time needed to reach a maximum concentration at a certain point in the skin. Additionally, *In vivo* studies of MONOCRYL plus sutures subcutaneously implanted along with *E. coli* and *S. aureus* show a 2 log reduction and 3.4 log reduction in bacterial concentrations when compared to un-impregnated sutures of the same material. (3)

## 8.0 Conclusions

The 2D model shows that the concentration of triclosan reached at the wound site is high enough for inhibition of bacterial growth. The concentration profile at the wound site peaks in the first 24 hours. Based on the results of this model, we suggest to surgeons using MONOCRYL plus sutures place them with a minimum 2 mm spacing in the skin for effective triclosan elution over 72 hours for the standard 4-0 MONOCRYL suture size and antibiotic concentration. In addition, we have created a chart based on bacterial strain and suture size that surgeons can use as a guide to evaluate the maximum spacing between sutures. We have also created predictive equations, based on our model, which surgeons could use to evaluate the spacing between sutures when trying to inhibit bacterial growth.

Our research has vast implications for medicine. Our recommendations may possibly change the way that surgeons and physicians add sutures to wounds. We have developed guidelines that, if implemented correctly and broadly, can considerably reduce morbidity and mortality of infections at the surgical site as well as the costs associated with such infections. Our model could also be extended to wounds not incurred during surgery.

## 9.0 Recommendations

Further research could look at sutures along wounds that are not straight incisions. The wound site would not necessarily be in the center of the suture, which could affect the recommended spacing of the sutures. The stitches could also be modified such that their depth into the skin is modified to be deeper or shallower. This would also affect the antibiotic concentrations at the wound site and could alter recommendations. Our model does not include the knot at the surface of the skin and assumes that the stitches are not continuous – both of which may affect antibiotic concentrations and wound closure. The model could also be expanded to subcutaneous tissue closure, where the entire suture is embedded in the body and modifications would be made to take into account the various tissue microclimates.

## Appendix A.

Table 3. Properties for modeling triclosan release from the suture in the skin.

| | |
|---|---|
| $D_{Triclosan\ in\ polyamide}$ | $1.12 \times 10^{-14}$ $m^2/s$ (15) |
| $D_{Triclosan\ in\ viable\ epidermis}$ | $4.167 \times 10^{-11}$ $m^2/s$ (16) |
| Initial Radius of Suture | $7.5 \times 10^{-5}$ m (7, 11, 12) |
| Rate Coefficient of triclosan Metabolism | $3.81944 \times 10^{-6}$ $mol/m^3/s$ (10) |
| Suture Degradation Rate | $7 \times 10^{-6}$ m/day (11) |
| Partition Coefficient | Log $P_{o/w}$ = 4.8 (17) |
| Initial triclosan concentration in suture | 4.612 $mol/m^3$ (12) |
| Initial triclosan concentration in skin | 0 $mol/m^3$ |

The rate coefficient of triclosan in the skin was developed from Moss *et al*. (1999) measurements of triclosan glucuronide and triclosan sulfate in human skin after dosing triclosan on the surface as a fraction of the original dose. Thus, we assumed a first order degradation rate based on the changes in both triclosan glucuronide and triclosan sulfate combined over time. Table 3 depicts all parameters used in our model.

## Appendix B.

To solve the algebraic equations, a direct MUMPS solver was used. The fully coupled solver was also direct. Time stepping was initially small, but increased at later times, as much of the change occurred in the first twenty-four hours, after which steady state was almost always achieved. Time stepping was chosen to keep computation time reasonable but still accurately demonstrate concentration changes. All tolerances were either calculated automatically or were default values in COMSOL.

In order to simplify the problem and minimize the amount of elements needed, the mesh convergence analysis was performed on the 2D boundary between the suture and the skin. Triangular elements were used, with a 'normal' mesh coarseness in both the suture in the skin and variations in the coarseness of the boundary mesh. Figure 15 shows that the mesh converges around 12,000 elements for both early and later time points. The analysis was performed by tracking the triclosan concentration just outside of the suture at 3 and 24-hour time points, as this concentration is likely to be affected by the mesh at the boundary. We chose the 12,000-element mark to continue with the rest of the project to ensure that the mesh was fine enough to accurately model the transport of the antibiotics through the suture and skin but would not take unnecessary computation time.

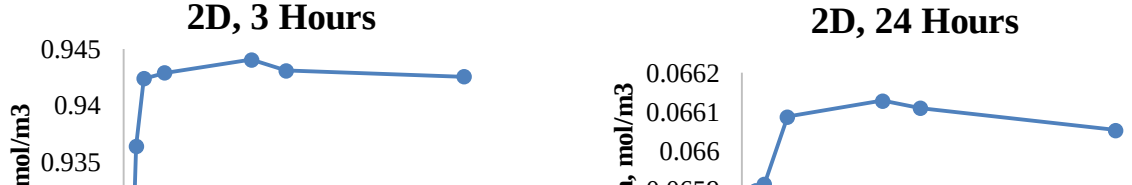

Figure 15. Mesh convergence of concentration just outside the suture, in 2D geometry with moving boundary condition and a partition coefficient. Solution appears to converge by 12,000 elements for both early time points (3 hours, left) and later time points (24 hours, right).

We performed a mesh convergence on the 3D model by varying the maximum element size along the boundary between the skin and the suture. The free tetrahedral elements in the mesh were set to 'normal' mesh density in the suture and the skin, and the number of elements was varied on the suture-skin boundary. Convergence was determined by calculating the triclosan concentration at a point just outside of the suture boundary (Figure 17A and 17B). According to the mesh profile (Figure 16), the model is accurately depicted with a minimum of 100,000 elements (Figure 17C). We used 100,000 elements to run the model. This corresponds to a maximum element size of 1E-5 m. We did not use an adaptive mesh, which may impact our results, given the fact that the skin-suture boundary is changing.

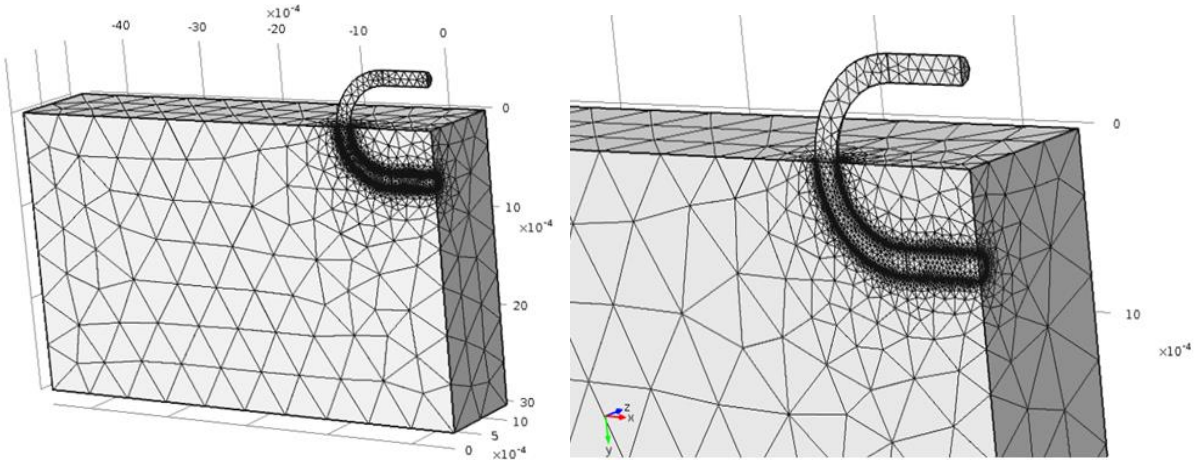

Figure 16. Mesh profile for 3D model at converged mesh element size displaying greatest mesh concentration at the suture boundary within the skin. Left panel depicts a zoomed out version of the 3D mesh, while right panel focuses on the suture boundary where the mesh is the densest.

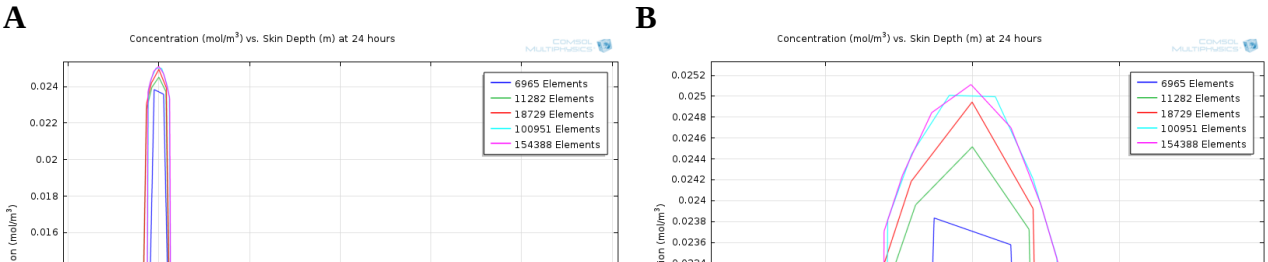

C

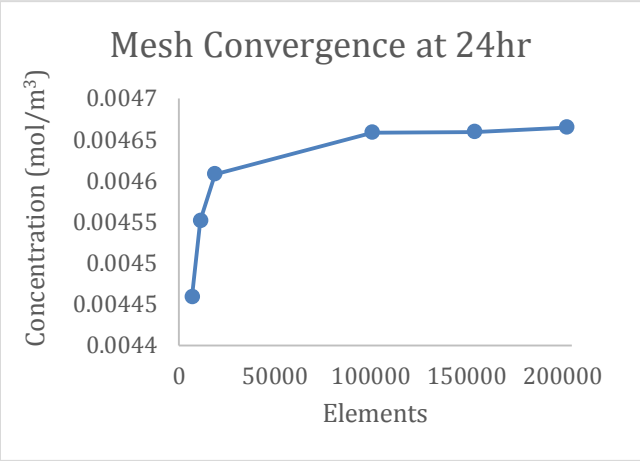


D

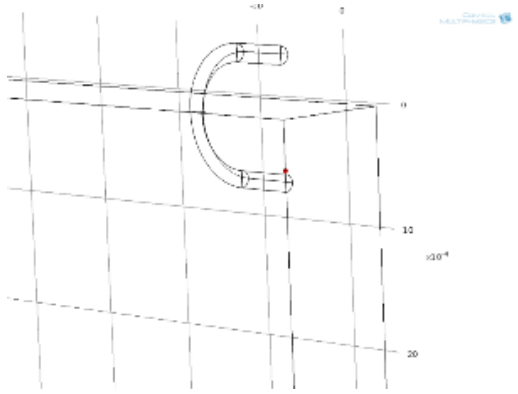

Figure 17. Mesh convergence in 3D geometry with moving boundary condition. Mesh convergence was calculated by examining the concentration along a line drawn through the center of the suture depth-wise into the skin. Mesh elements are concentrated at suture boundary A) At the 24 hour time point, the mesh converges around 100,000 elements. B) Zoomed-in view. C) Concentration vs. number of elements at point D) just outside of the suture.

As shown in Figure 16 and Figure 17, we reduced discretization error through mesh convergence in our model.

**Appendix C.**

To depict multiple stitches in the skin, we generated mirror plots showing changes in concentration of triclosan in a realistic image of multiple stitches, as they would appear after implementation in the wound (Figure 18).

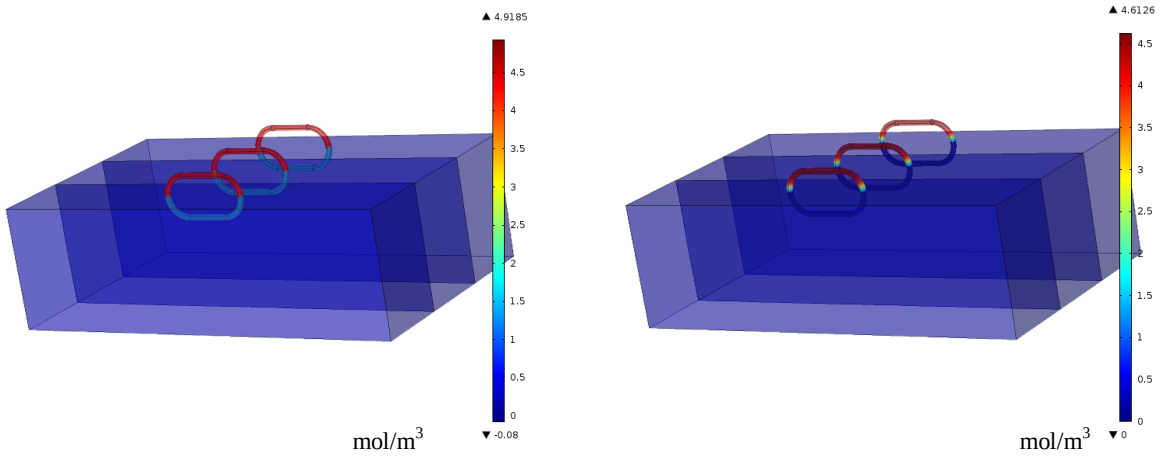


Figure 18. Concentration surface mirror plots for 3D model showing three stitches along a wound site. A) At initial time (t=0). B) After 24 hours.

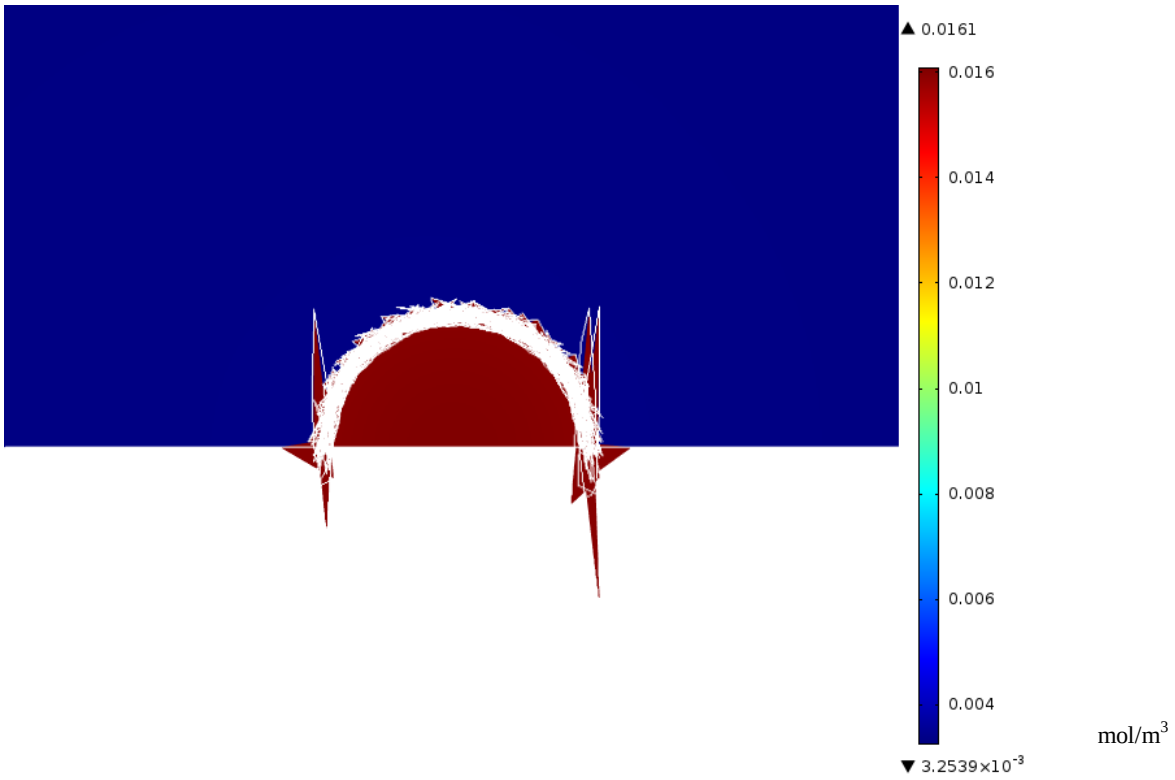


Figure 19. Mesh inversion that took place at later timepoints (after 120 hours) in both 2D and 3D models before correction.

Before correction, both of our 2D and 3D models showed mesh inversion at later timepoints (Figure 19). This was corrected in the 3D model to ensure accurate measurements of stitch volume after 7 days. All other computation was performed before the mesh began to invert.

**Appendix D. References**


1. Wang, ZX, Jiang, CP, Cao, Y, & Ding, YT. (2013). Systematic review and meta-analysis of triclosan-coated sutures for the prevention of surgical site infection. *British Journal of Surgery* 100, 465-473.

2. Edmiston, C. E. , Seabrook, G. R., Goheen, M. P. , Krepel, C. J. , Johnson, C. P. , Lewis, B. D., Brown, K. R., & Towne, J. B. (2006). Bacterial adherence to surgical sutures: can antibacterial-coated sutures reduce the risk of microbial contamination? *Journal of American College of Surgeons*, 203(4), 481-489.

3. Ming, X., Rothenburger, S., Yang, D. (2007). In vitro antibacterial efficacy of MONOCRYL plus antibacterial suture (poliglecaprone 25 with triclosan). *Surgical Infections*, 8(2), 201-207.

4. Al-Mubarak, L., & Al-Haddab, M. (2013). Cutaneous Wound Closure Materials: An Overview and Update. *Journal of Cutaneous and Aesthetic Surgery*, *6*(4), 178–188. doi:10.4103/0974-2077.123395

5. Osterberg, B., & Blomstedt, B. (1979). Effect of suture materials on bacterial survival in infected wounds. An experimental study. *Acta Chirurgica Scandinavica*, *145*(7), 431–434.

6. Bezwada, RS, Jamiolkowski, DD, Lee, I et al. (1995). Monocryl suture, a new ultra pliable absorbable monofilament suture. *Biomaterials* 16, 1141-1148.

7. Molea, G, Schonauer, F, Bifulco, G & D'Angelo, D (2000). Comparative study on biocompatibility and absorption times of three absorbable monofilament suture materials (Polydioxanone, Poliglecaprone 25, Glycomer 631). *British Journal of Plastic Surgery* 53, 137-141.

8. Chu CC, von Fraunhofer JA, Griesler HP. Wound Closure Biomaterials and Devices. *CRC Pres.* 2013.

9. Jones Gl, Muller CT, O'Reilly M, Stickler DJ. (2006) Effect of triclosan on the development of bacterial biofilms by urinary tract pathogens on urinary catheters. *Journal of Antimicrobial Chemotherapy* 57:266-72.

10. Moss, T., Howes, D. & Willaims, F. M. (1999). Percutaneous penetration and Dermal Metabolism of Triclosan. *Food and Chemical Toxicology* 38, 361-370

11. Lyu, S., & Untereker, D. (2009). Degradability of polymers for implantable biomedical devices. *International Journal of Molecular Sciences* 10, 4033-4065.

12. Food and Drug Administration. (2005). http://www.accessdata.fda.gov/cdrh_docs/pdf5/K050845.pdf. Accessed 2/13/14.

13. Leaper, D. (1994). Prophylactic and therapeutic role of antibiotics in wound care. *American*

*Journal of Surgery.* 167(1A): 15S-19S.

14. Lendlein, A., Langer R (2002). Biodegradable, elastic shape-memory polymers for potential biomedical applications. *Science,* 296(5573): 1673-1676.

15. Zurita, R., Puiggali, J., Rodriguez-Galan, A. (2006) Triclosan release from coated polyglycolide threads. *Macromolecular Bioscience* 6: 58 – 69.

16. Kruse, J., Golden, D., Wilkinson, S., Williams, F., Kezic, S., & Corish, J. (2007). Analysis, Interpretation, and Extrapolation of Dermal Permeation Data Using Diffusion-Based Mathematical Models. *Journal of Pharmaceutical Sciences* 96 (3): 682-703.

17. Scientific Committee on Consumer Products. (2009). Opinion on Triclosan. *European Commission 2009.*

**Appendix G.**

| Team member name | Caitlin | Calvin | Garrett | Beth | NOT DONE |
|---|---|---|---|---|---|
| Wrote abstract | x | | | | |
| Edited abstract | x | x | | x | |
| Wrote introduction | x | x | x | x | |
| Edited introduction | x | x | x | x | |
| Wrote method section | x | x | | x | |
| Edited method section | x | x | x | x | |
| Wrote results section | x | x | x | x | |
| Edited results section | x | x | x | x | |
| Wrote discussion section | x | x | x | x | |
| Edited discussion section | x | x | x | x | |
| Wrote summary and conclusion section | x | | | | |
| Edited summary and conclusion section | x | x | x | x | |
| Wrote bibliography section | x | x | | | |
| Edited bibliography section | x | x | | x | |
| Prepared processed data table for appendix | x | x | x | x | |
| Checked data in processed data table in appendix | x | x | x | x | |
| Prepared figures or tables for main text | x | x | x | x | |
| Checked figures or tables in main text | x | x | x | x | |
| Assigned tasks to group members | x | x | | x | |
| Put the report together from the parts provided by | x | | | x | |

| | | | | | |
|---|---|---|---|---|---|
| others | | | | | |
| Read and edited entire document to check for consistency | x | x | x | x | |